

비대칭 하중 섬유강화 복합재의 동적 파괴 해석 페리다이나믹 모델

Peridynamic models for dynamic fracture in an asymmetrically loaded unidirectional composite

Wenke Hu*, 하 윤 도**, Florin Bobaru***
Hu, Wenke • Ha, Youn Doh • Bobaru, Florin

Abstract

We use a recently introduced peridynamic computational model of fiber-reinforced composites to replicate a famous experiment by Coker and Rosakis (2001) in which intersonic crack growth is observed in asymmetrically loaded unidirectional composite plates. The peridynamic model is able to capture the straight crack growth from an asymmetric loading of the composite. Compared to the symmetric loading, the asymmetric loading leads to a much higher propagation velocity. The results show the formation of a shock wave similar to that reported in the experiments.

keywords : dynamic fracture, crack propagation, fiber-reinforced composites, peridynamics, intersonic cracks

1. Introduction

Significant efforts have been made to model damage and failure in FRCs based on classical elasticity, the Finite Element Method and damage or fracture models (mostly under quasi-static loading). In Guimard, 2009, such treatments of fracture in composites require prior knowledge of the actual fracture modes and of the crack paths. In dynamic loading conditions the fracture modes and the crack paths are unknown in advance and thus, these classical models cannot be very useful except in special situations. As indicated by dynamic experiments on unidirectional (UD) fiber-reinforced composites (FRCs) Haque, 2005, different failure modes may coexist and are coupled in dynamic fracture of UD FRCs. The dynamic interactions among matrix cracking, splitting, delamination and stress waves determine the dynamic fracture and failure behavior in such composites. The homogenized peridynamic model introduced in Hu, 2011 and Hu, 2012 was shown to obtain the crack paths, and their kinetics as part of the solution, and at the same time allow for the autonomous interaction between stress waves, cracks, and fracture modes. In contrast to the results expected from quasi-static loading, the simulations in Hu, 2012 showed that dynamic conditions can lead to co-existence of and transitions between fracture modes in which matrix shattering can happen before a splitting crack propagates. Matrix-fiber splitting fracture, matrix cracking,

* University of Nebraska-Lincoln, USA 박사과정

** 정회원 • 군산대학교 조선공학과 전임강사 ydha@kunsan.ac.kr

*** University of Nebraska-Lincoln, USA 부교수 fbobaru2@unl.edu

and crack migration in the matrix, including crack branching in the matrix similar to what was observed in recent dynamic experiments (Haque, 2005) is correctly shown by the peridynamic simulations. Notice that in peridynamics no special criteria are needed for splitting mode fracture, crack curving, or crack arrest. All these modes of material failure are obtained as a direct result of the peridynamic solution.

2. Review of the Peridynamics Formulation

The peridynamic theory uses an integral of forces acting at a point over a certain nonlocal region around the point (δ) instead of the divergence of stresses term in the classical equations of motion (Silling, 2000). Therefore, this formulation is well suited for modeling problems in which displacement discontinuities emerge, interact, and evolve in time. The peridynamic equations of motion are:

$$\rho \ddot{\mathbf{u}}(\mathbf{x}, t) = \int_H \mathbf{f}(\mathbf{u}(\hat{\mathbf{x}}, t) - \mathbf{u}(\mathbf{x}, t), \hat{\mathbf{x}} - \mathbf{x}) d\hat{\mathbf{x}} + \mathbf{b}(\mathbf{x}, t) \quad (1)$$

where \mathbf{f} is a pairwise force in peridynamic bond connecting $\hat{\mathbf{x}}$ to \mathbf{x} , and \mathbf{u} is the displacement vector field. ρ and \mathbf{b} are the mass density and the body force, respectively. The integral is defined over a region H called the "horizon" taken by δ . A micro-elastic material is defined as one for which the pairwise force derives from a micro-potential ω as $\mathbf{f}(\boldsymbol{\eta}, \boldsymbol{\xi}) = \partial \omega(\boldsymbol{\eta}, \boldsymbol{\xi}) / \partial \boldsymbol{\eta}$ where $\boldsymbol{\xi}$ and $\boldsymbol{\eta}$ are the relative position and relative displacement of points $\hat{\mathbf{x}}$ and \mathbf{x} in the reference configuration. A "linear" micro-elastic potential is used as $\omega(\boldsymbol{\eta}, \boldsymbol{\xi}) = c(\boldsymbol{\xi}) s^2 \|\boldsymbol{\xi}\| / 2$ where s is the bond relative elongation $s = (\|\boldsymbol{\eta} + \boldsymbol{\xi}\| - \|\boldsymbol{\xi}\|) / \|\boldsymbol{\xi}\|$. The corresponding pairwise force becomes

$$\mathbf{f}(\boldsymbol{\eta}, \boldsymbol{\xi}) = \frac{\partial \omega(\boldsymbol{\eta}, \boldsymbol{\xi})}{\partial \boldsymbol{\eta}} = c(\boldsymbol{\xi}) s \|\boldsymbol{\xi}\| \frac{\partial s}{\partial \boldsymbol{\eta}} = c(\boldsymbol{\xi}) s \frac{\partial \|\boldsymbol{\xi} + \boldsymbol{\eta}\|}{\partial \boldsymbol{\eta}} \quad (2)$$

The function $c(\boldsymbol{\xi})$ is called the micromodulus function and represents the bond elastic stiffness. For isotropic materials, the micromodulus function is computed by matching the peridynamic strain energy to the classical strain energy. In this paper we used the conical micromodulus as given in Ha, 2010.

3. The scaled discrete peridynamic model for arbitrary fiber orientation relative to the discretization grid

In Hu, 2011 we used the model with a uniform grid aligned with the fiber directions and performed calculations on a 0° lamina with a center crack perpendicular to the fiber direction. A certain scaling of the micromodulus was necessary in order to keep the strain energy density from the discretized homogenized peridynamic model the same under grid refinement (see table 2 in Hu, 2011). The scaled discrete version of the conical micromodulus function for the continuum anisotropic peridynamic model is:

$$C^d(\boldsymbol{\xi}, \theta) = \begin{cases} \lambda_{fb} c_{11}^i(\boldsymbol{\xi}) & \text{if } \theta = 0 \text{ or } \pi \\ \lambda_{mb} c_{22}^i(\boldsymbol{\xi}) & \text{otherwise} \end{cases} \quad (3)$$

$$c_{11}^i(\boldsymbol{\xi}) = \frac{12(E_{11} + \nu_{12}E_{22})}{(1 - \nu_{12}\nu_{21})\pi\delta^3} \left(1 - \frac{\boldsymbol{\xi}}{\delta}\right), c_{22}^i(\boldsymbol{\xi}) = \frac{12(E_{22} + \nu_{12}E_{11})}{(1 - \nu_{12}\nu_{21})\pi\delta^3} \left(1 - \frac{\boldsymbol{\xi}}{\delta}\right) \quad (4)$$

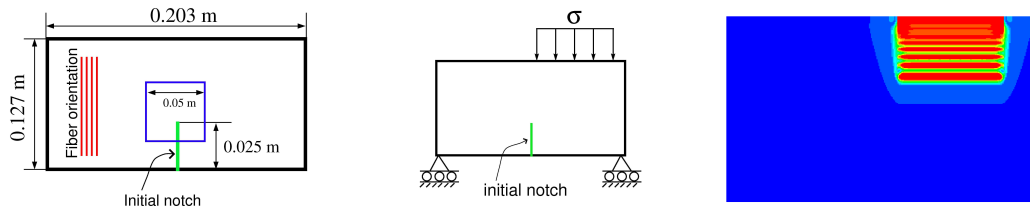
with λ_{fb} and λ_{mb} being dimensionless scaling factors corresponding to the "fiber bonds" and the "matrix bonds" (Hu, 2011). These scaling factors do not apply for the case when the uniform discretization grid

is not aligned with the fiber orientation or for the case of non-uniform discretizations. A proper scaling is needed therefore to keep the strain energy density independent of the fiber orientation relative to the grid orientation. For an arbitrary orientation of the grid relative to the fibers and/or when a non-uniform discretization is used, there might not be any nodes exactly sitting along the fiber direction that passes through the center node. Since finding exact scaling factors are not easy in these cases, we obtain appropriate values of them numerically (Hu, 2012). More details are given in Hu, 2012.

4. Problem setup and numerical results

We consider the following setup for analyzing dynamic fracture phenomena in a UD FRC (the same set up as in Coker, 2001): an edge-notched thin rectangular plate as shown in Fig. 1-a. Asymmetric loading (which induces fracture mode II) is applied suddenly to the sample (Fig. 1-b) and maintained constant afterwards. In the experiments of Coker, 2001, the impulsive loading is provided by impact with a fast projectile. In our simulations, the loading magnitude is 40MPa. We noticed that higher amplitude loadings produced more significant damage while lower amplitude loading (such as 25MPa) induces a crack that turns before running like a splitting straight crack. This is due to the particular wave interactions around the tip of the pre-notch and the stress intensity reached before propagation. In our simulations we impose the displacement conditions shown in Fig. 1. The dynamic experiments in UD FRC with this type of loading reported in Coker, 2001 show that cracks can propagate at intersonic speeds.

The composite material used in the example shown below is the graphite/epoxy (Coker, 2001). Young's moduli are 80 GPa (longitudinal E_{11}) and 8.9 GPa (transverse E_{22}). Shear modulus G_{12} is 3.6 GPa. Poisson ratio ν_{12} is 0.25 and density is 1478 kg/m³. Also, fracture energy along transverse direction is 0.168 kJ/m². In the computations we used a horizon size of 3 mm and the ratio between the horizon size and the grid spacing, the parameter m , is taken here to be 5.



(a) Geometry of UD FRC specimen (b) asymmetric loading condition (c) plot of strain energy density

Figure 1 Problem setup: (a) the blue square represents the region for which the results in Fig. 3 are presented, (c) notice the trailing waves due to the nonlocal dispersion of wave front.

The results in Fig. 2-(a-c) show the evolution of the crack growth. The shock wave hits the pre-notch tip before 2 μ s but the crack does not start to propagate until around 9 μ s after a set of waves create a sufficiently high stress intensity factor around the crack tip. The crack grows parallel to the fibers in a splitting mode. This is also observed in the experiments of Coker, 2001. The estimated crack propagation speed (see Fig. 2-d) indicates that the crack growth accelerates rapidly and at some point becomes intersonic. Around 15 μ s a certain shock wave (with an angle of about 18-20 degrees) can be distinguished from Fig. 2-c. A similar behavior is observed in the experiments. The speed

reached by the crack computed by the peridynamics simulation is larger than that measured in the experiments, which is around 7000–8000m/s. This is to be expected since here we used a relatively large nonlocal region (horizon) due to limited computational resources. As shown in Hu, 2011, with a horizon slightly below 1 mm we would be able to match the propagation behavior not only qualitatively but also quantitatively. This is planned for the future. We have also performed computations for the symmetrical loading conditions and, as reported in the experiments, the crack propagation speed is significantly lower than in the asymmetrical loading. With a horizon of 3 mm we obtain a maximum propagation speed of around 4000m/s. We expect that with a horizon of around 1mm (see Hu, 2011) the maximum speed will be close to that measured in Coker, 2001.

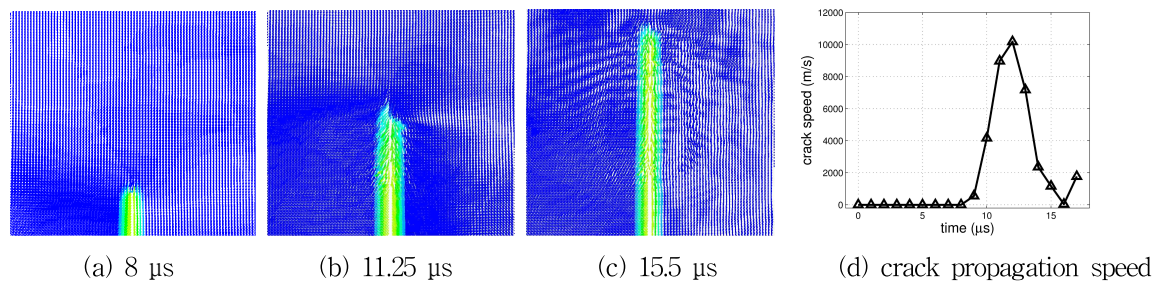


Figure 2. (a–c) a selected sequence of quiver plots of velocity vectors and damage maps for the crack propagation under asymmetric loading for the region in the blue square of Fig. 1. (d) crack propagation speed

5. Conclusions

We have employed a homogenized peridynamic model for unidirectional fiber-reinforced composites to simulate intersonic crack propagation in such a material loaded in an asymmetric way. The model is capable of reproducing the dynamic crack growth characteristics reported in the experiments of Cocker, 2001. To the best of our knowledge, this is the first time a computational model is able to predict intersonic crack growth in asymmetrically loaded unidirectional composites.

Acknowledgements

The authors are thankful for the financial support offered through research contracts between UNL and the ARO (Dr. Larry Russell), and ARL (project coordinators Dr. C.F. Yen and Dr. C. Randow), ARO proposal number 58450EG. The work of YD Ha was also supported by research funds from Kunsan National University.

참고문헌

- Coker, D., Rosakis, A.J. (2001) Experimental observations of intersonic crack growth in asymmetrically loaded unidirectional composite plates. *Philosophical Magazine A*, 81(3), pp.571–595.
- Guimard, J.M., Allix, O., Pechnik, N., Pascal, T. (2009) Characterization and modeling of rate effects in the dynamic propagation of mode-II delamination in composite laminates. *Int J Fract*, 160, pp.55–77.
- Ha, Y.D., Bobaru, F. (2010) Studies of dynamic crack propagation and crack branching with peridynamics, *Int J Fract*, 162, pp. 229–244.
- Ha, Y.D., Bobaru, F. (2011) Characteristics of dynamic brittle fracture captured with peridynamics, *Eng Fract Mech*, 78, pp.1156–1168.
- Haque, A., Ali, M. (2005) High strain rate responses and failure analysis in polymer matrix composites—an experimental and finite element study. *J Compos Mater*, 39, pp.423–450.
- Hu, W., Ha, Y.D., Bobaru, F. (2011) Modeling dynamic fracture and damage in fiber-reinforced composites with peridynamics. *Int J Multiscale Computational Engineering*, 9, pp.707–726.
- Hu, W., Ha, Y.D., Bobaru, F. (2012) Peridynamic model for dynamic fracture in unidirectional fiber-reinforced composites, *Comput Method Appl Mech Eng*, 217–220, pp.247–261.
- Silling, S.A. (2000) Reformulation of elasticity theory for discontinuities and long-range force, *J Mech Phys Solids*, 48, pp. 175–209.